



**Titel** A Muon Beam Profile Monitor With Scintillating Fiber Readout by Avalanche Microchannel Photodiodes (AMPDs)

Ersetzt

**Autoren / Autorinnen** A. Stoykov, R. Scheuermann, Th. Prokscha, Ch. Buehler, Z. Sadygov\*

Erstellt

21.12.2004

**Zusammenfassung:**

A position-sensitive detector (the Muon Beam Profile Monitor -  $\mu$ BPM) for non-relativistic muon beams and to be used in high magnetic fields was developed. The  $\mu$ BPM consists of a grid of 10+10 scintillating fibers probing the muon beam intensity along the horizontal (X) and the vertical (Y) direction perpendicular to the beam direction (Z), i.e., at  $X_i$  and  $Y_j$  coordinates of the fibers ( $i, j = 1 \dots 10$ ). The readout of the fibers is realized by avalanche microchannel photodiodes (AMPDs). The usage of AMPDs results in a compact design of the device, its insensitivity to magnetic fields, and the ability to handle high event rates.

The  $\mu$ BPM was successfully utilized in the measurement of the muon beam profiles in magnetic fields up to 4.8 Tesla and at event rates as high as  $3 \cdot 10^6 \text{ s}^{-1}$  per channel.

\* Veksler and Baldin Laboratory of High Energies, Joint Institute for Nuclear Research, 141980 Dubna, Moscow region, Russia

Verteiler	Abt.	Empfänger / Empfängerinnen	Expl.	Abt.	Empfänger / Empfängerinnen	Expl.		Expl.
	3511	A. Amato	1				Bibliothek	
	3000	R. Bercher	3				Reserve	
	3000	K. Clausen	1				Total	
	8580	K. Deiters	1				Seiten	
	3500	D. Herlach	1				Beilagen	
	3512	E. Morenzoni	1				Informationsliste	
	1412	D. Renker	1				D 1 2 3 4 5 8 9 A	
	1414	N. Schlumpf	1				Visum Abt./Laborleitung:	



A position sensitive detector capable to measure the profile of a non-relativistic muon beam and operational in high magnetic fields is essential for the set-up and optimization of the performance of  $\mu$ SR spectrometers, such as the Avoided Level Crossing (ALC)  $\mu$ SR spectrometer [1] or the planned High – Magnetic Field (HMF)  $\mu$ SR-spectrometer (up to 10 T).

The ALC  $\mu$ SR spectrometer accommodated in area  $\pi$ E3 is regularly used to study the properties of condensed matter via the observation of the loss of integrated muon spin polarization at the avoided crossing of quantised magnetic energy levels in high magnetic fields [2]. The basic part of the spectrometer is a superconducting solenoid with a room-temperature bore of 20 cm diameter and a length of 1 m, which creates a longitudinal (with respect to the initial muon spin polarization) magnetic field up to 5 Tesla at the center. The polarization of muons stopped in a sample is determined by the registration of decay positrons in two detector sets located up- and downstream with respect to the muon beam direction. The quality of an ALC spectrum (field dependence of the measured muon spin polarization) strongly depends on the position and the size of the muon beam spot on the sample as this affects as well the solid angle of positron registration and the effective decay positron trajectory (due to spiraling of the charged particles in a magnetic field). To measure the muon beam profile at the solenoid center and its dependence on the beamline settings and the magnetic field a Muon Beam Profile Monitor ( $\mu$ BPM) was designed and built.

The  $\mu$ BPM (see Fig. 1) consists of a grid of twenty scintillating fibers with round cross section ( $\varnothing$  1 mm, POLIFI 0244-100 [3], peak emission at  $\lambda \approx 440$  nm). Ten fibers are spaced along the X axis, and ten along the Y axis (the two orthogonal directions perpendicular to the muon beam direction Z). The length of the fibers and the spacing are 100 mm and 10 mm, respectively. The diameter of 1 mm is chosen as approximately half the range of a muon with a momentum of 29 MeV/c. A muon passing through a fiber (or even stopped inside) produces scintillation light which is registered at one end of the fiber by an avalanche microchannel photodiode (AMPD) [4] of type Dubna R8 (the basic characteristics are shown in Table 1). Each AMPD is mounted on the printed board of a preamplifier minimizing the distance from the AMPD pins to the electric circuit. The supply voltage for the preamplifiers and the bias voltage for the AMPDs are distributed by one motherboard for each direction (X and Y). The scintillating fibers and the motherboards with the AMPD – preamplifier boards are mounted on an aluminium frame with dimension 100 x 100 mm<sup>2</sup>. The  $\mu$ BPM probes the beam intensities  $I_i$  and  $I_j$  over each individual fiber at the coordinates of the fibers  $X_i$  and  $Y_j$ ,  $i, j = 1 \dots 10$ .

The choice of an AMPD as photosensor for the  $\mu$ BPM is conditioned by its high photon detection efficiency and its high gain. The high gain of the AMPD allows to use a fast voltage-sensitive preamplifier, which is an essential requirement at high ( $> 10^6 \text{ s}^{-1}$ ) event rates. The electrical scheme combining the AMPD biasing and the amplifier circuits is shown in Figure 2.

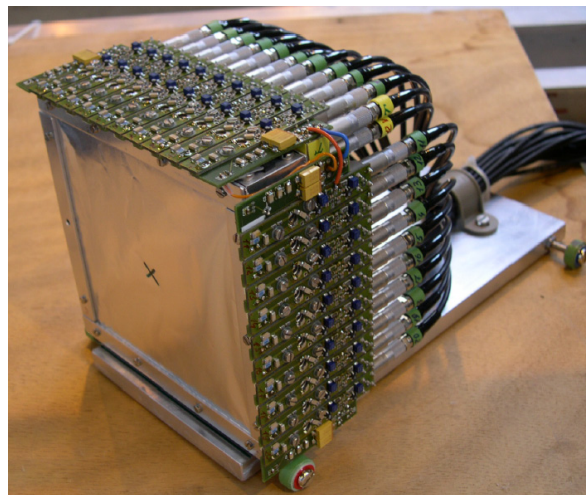
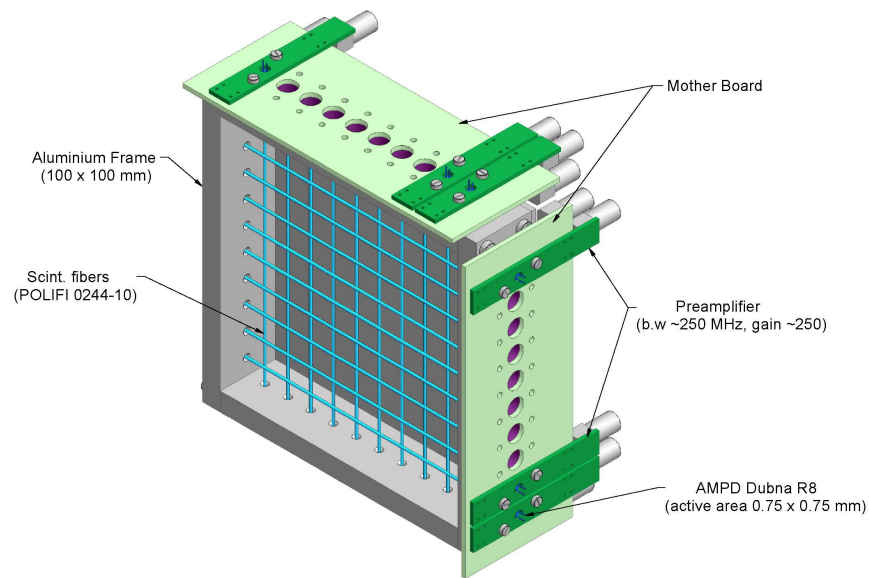


Figure 1: Design (top) and actual (bottom) views of the Muon Beam Profile Monitor.

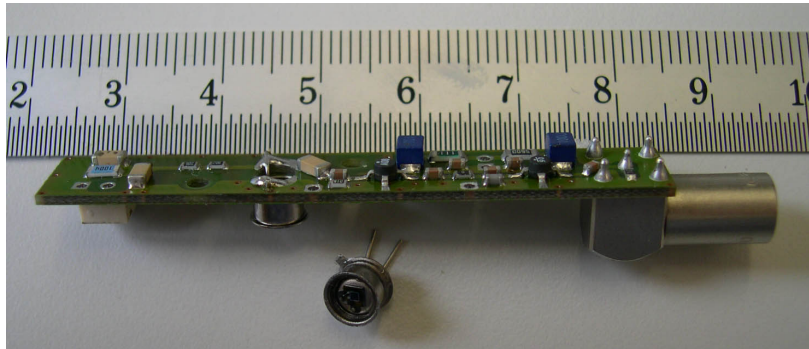
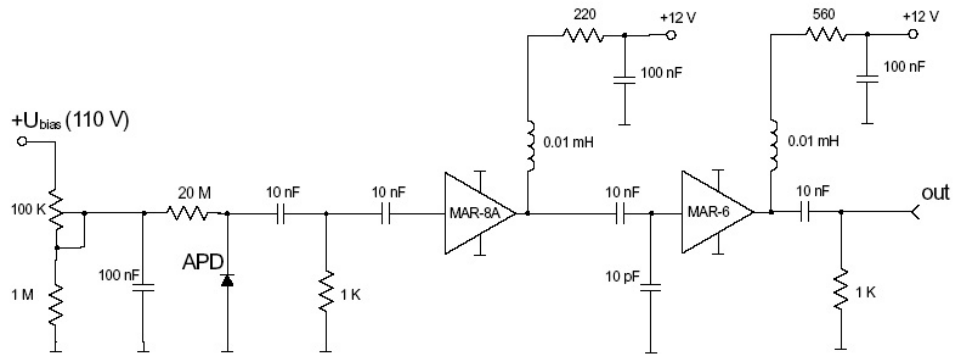


Figure 2: Top: AMPD biasing and amplifier circuits. Bandwidth and gain of the amplifier are  $\sim 250$  MHz and  $\sim 250$ , respectively. Bottom: AMPD mounted on preamplifier board.

Photosensitive area	$0.75 \times 0.75 \text{ mm}^2$
Quantum Efficiency at 440 nm	$\sim 60\%$
Photon Detection Efficiency at 440 nm	$\sim 15\%$
Maximum gain ( $M_{\max}$ )	$5 \cdot 10^4$
Dark current at $M_{\max}$	$\sim 200 \text{ nA}$
Operating voltage	$\sim 100 \text{ V}$

Table 1: Basic characteristics of the AMPD type Dubna R8

A common voltage source (KEITHLEY picoammeter 6487) was used for biasing all the AMPDs. The bias voltage for each channel was adjusted individually by means of an on-board voltage divider. The 20 M $\Omega$  value of the biasing resistor was chosen to minimize the effect of temperature variations on the AMPD gain. The disadvantage of such a large serial resistance is that at a rate of  $\sim 10^6$  s $^{-1}$  the signal amplitude drops by a factor of two compared to its value at lower ( $< 10^5$  s $^{-1}$ ) muon rates. For the commissioning of the new  $\mu$ E4 beam the value of the biasing resistor was changed to 20 k $\Omega$  which allowed measuring rates as high as  $3 \cdot 10^6$  muons/sec. The preamplifier scheme is based on MAR monolithic amplifiers from Mini-Circuits [5]. It has a gain of  $\sim 250$  over a bandwidth of  $\sim 250$  MHz. Due to the high gain of the AMPD the amplitudes of  $1 e^-$ -pulses were much larger than the amplifier noise level, so that signals corresponding to one or two thermally generated electrons (differing by a factor of two in amplitude) were clearly visible on an analog oscilloscope ( $1 e^-$ -signals can even be well distinguished on a digital scope, see Fig. 3). During the operation the power dissipation in the amplifier circuits lead to an increase of the temperature of the whole aluminum frame to about 50  $^{\circ}$ C as measured by sensors mounted on the motherboards.

The analog output signals from the amplifiers were sent via 40 m long low-loss cables to the input of constant fraction discriminators (ORTEC CFD935 or PSI prototype CFD105/950) with the trigger level of about 25 – 30 mV for each of the channels. ECL signals from the CFDs (formed directly by the CFD105/950 or obtained via a NIM/ECL converter in the case of the CFD935) then were fed to

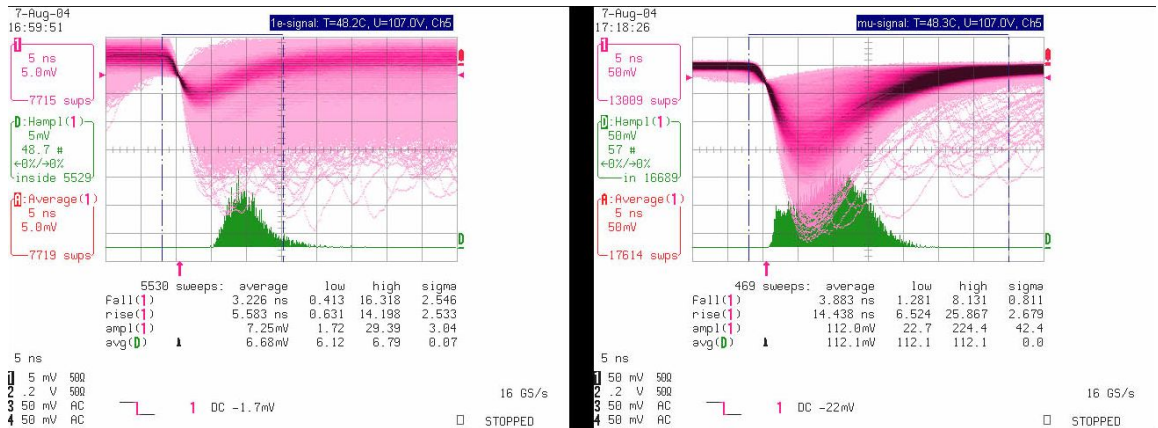


Figure 3: Oscilloscope (LeCroy "WavePro 960") images for the dark ( $1 e^-$ ) and  $\mu^+$ -signals from the channel X5 (the light collection for this channel was the lowest among all channels).

a 32 channel 32-bit 250 MHz VME scaler SIS3820. The scalers were run over a predefined time interval and the accumulated counts were used to calculate the X and Y projections of the beam.

The waveforms and the amplitude distributions of the  $\mu$ BPM output signals were analyzed using a LeCroy "WavePro 960" digital oscilloscope. Figure 3 shows the oscilloscope images obtained for the dark ( $1e^-$ ) and  $\mu^+$ -pulses from one of the BPM channels (channel X5). Figure 4 shows the amplitude distributions of the  $1e^-$ - and  $\mu^+$ -signals for the channels X5 and X6. The bias voltage for each of the twenty channels was adjusted to an approximately equal ( $7 - 8$  mV) amplitude of  $1e^-$ -signals in each channel. However, due to different light collection efficiencies in the individual channels (mainly caused by a variation of the distance between AMPD and fiber in the order of a few  $100 \mu\text{m}$ ), the  $\mu^+$ -signal amplitudes varies between different channels. The channels X5 and X6 were the ones with the minimum and the maximum light collection efficiencies: the most probable amplitudes of the muon signals for these channels were about 16 and 30 photoelectrons, respectively. The signal amplitudes for the other channels were within this range.

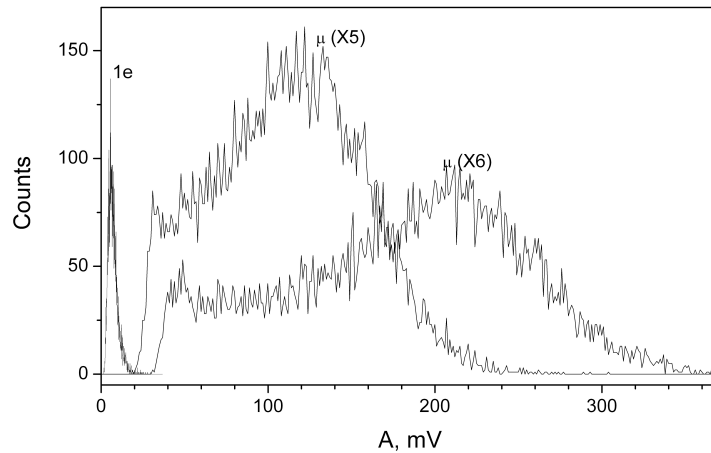


Figure 4: Amplitude distributions of  $\mu^+$ -signals for channels X5 (minimum light collection; the most probable amplitude  $A_\mu$  corresponds to  $\approx 16$  photoelectrons) and X6 (maximum light collection;  $A_\mu \approx 30$  phe). The most probable amplitude of the dark ( $1e^-$ ) pulses is  $7 - 8$  mV for each of the twenty channels.

The variation of the light collection and gain in the individual channels results in a variation of the detection efficiencies and therefore might influence the mea-

sured horizontal and vertical muon beam profiles. The stability of the measured distributions was checked over a certain variation of gain. The gain of an AMPD increased by a factor of 2.5 as the bias voltage was varied from 103.0 V to 107.0 V. The rate of dark counts at a given threshold level (about 30 mV) changed from 0 to  $3000 \text{ s}^{-1}$  in the above range of  $U_{\text{bias}}$  (see Fig. 5). A dark count rate in the order of  $10^3 \text{ s}^{-1}$  was considered as tolerable since the muon rate was at least one order of magnitude higher. Figure 6 shows the X-distributions of the muon beam spot obtained at different values of  $U_{\text{bias}}$ : the distributions are practically the same at  $U_{\text{bias}} \geq 104.00 \text{ V}$ .

The  $\mu\text{BPM}$  was used to measure the field dependence of the position and the size of the muon beam spot at the center of the ALC solenoid. Two-dimensional plots obtained by multiplying the X and Y distributions  $w_i w_j = I_i I_j / \sum I_i \sum I_j$  as shown in Figure 7 illustrate the muon beam-spot variation with the magnetic field. (For the purpose of visualization, no significant difference was found to 2D-plots constructed from coincidence measurements:  $w_{ij} = I_{ij} / \sum I_{ij}$ , where  $I_{ij}$  are the intensities of coincidences between the  $X_i$  and  $Y_j$  channels). The dependencies of  $\sigma_x$  and  $\sigma_y$  (the standard deviations for the X- and Y-distributions) on the magnetic field  $H$  are shown in Figure 8. The beam spot size oscillates with increasing magnetic field – a focusing effect of high magnetic fields. The beam spot position practically does not change with  $H$  as an effect of a lead collimator (diameter: 30 mm): without the collimator the mean values of the distributions depend on  $H$  and the field dependences of the beam projections  $\sigma_x(H)$ ,  $\sigma_y(H)$  are shifted in phase.

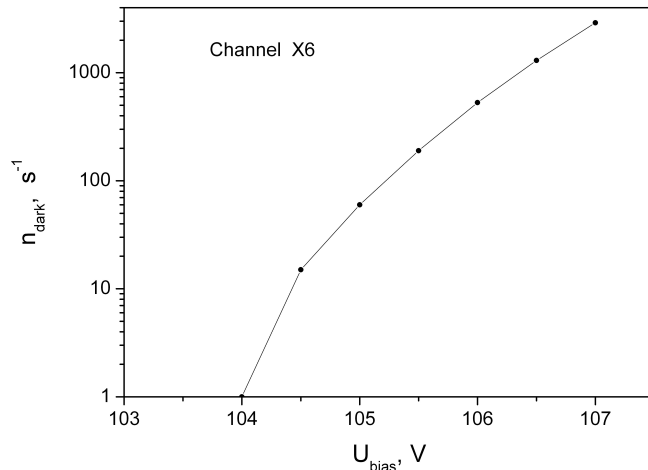


Figure 5: Dark count rates for channel X6 vs.  $U_{\text{bias}}$ . In the range  $103.00 \leq U_{\text{bias}} \leq 107.00 \text{ V}$  the AMPD gain changes by a factor of 2.5.



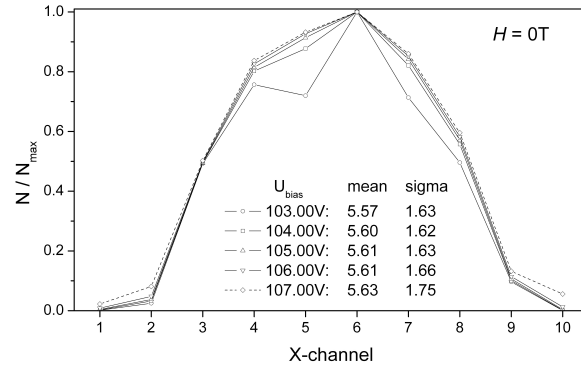


Figure 6: The X-distributions of the muon beam spot at zero field obtained at different values of  $U_{\text{bias}}$ .

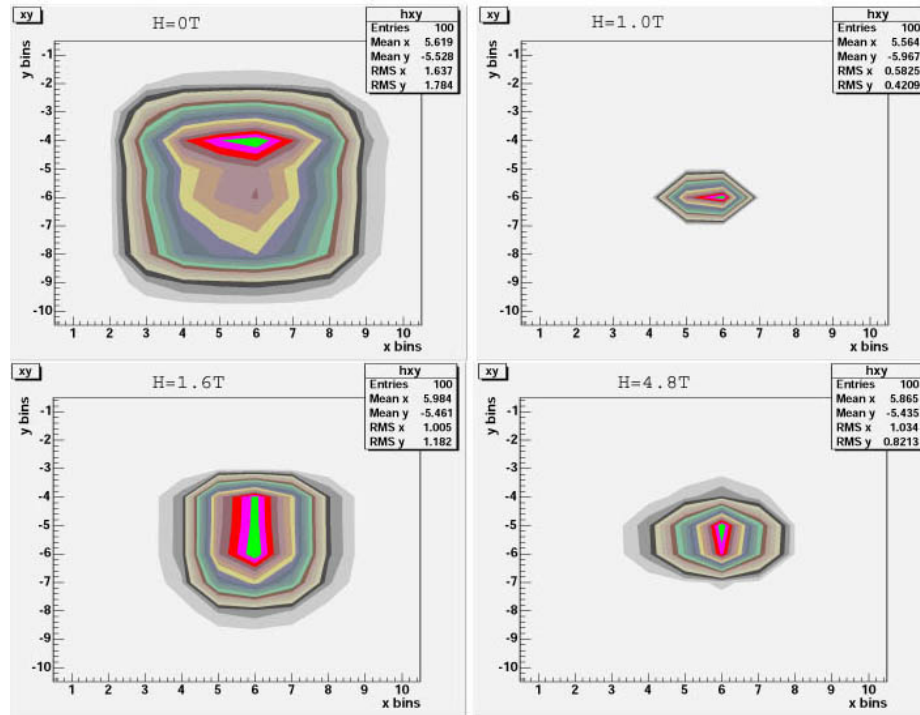


Figure 7: Two-dimensional plots (obtained by multiplying X- and Y-distributions) illustrate the change of the muon beam-spot with the magnetic field. The direction of view coincide with that of the muon beam.

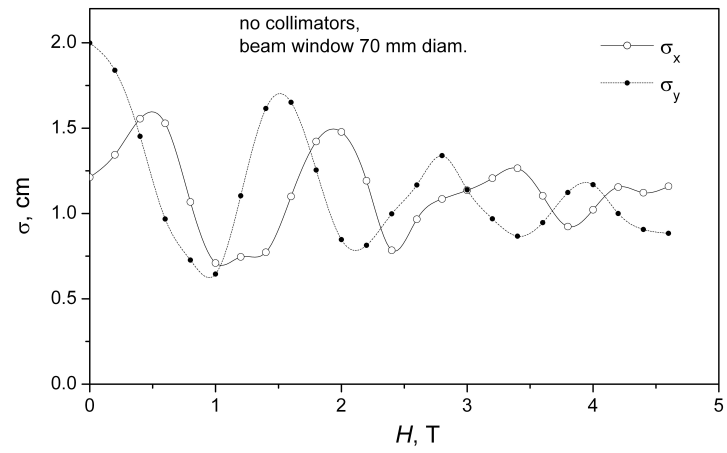
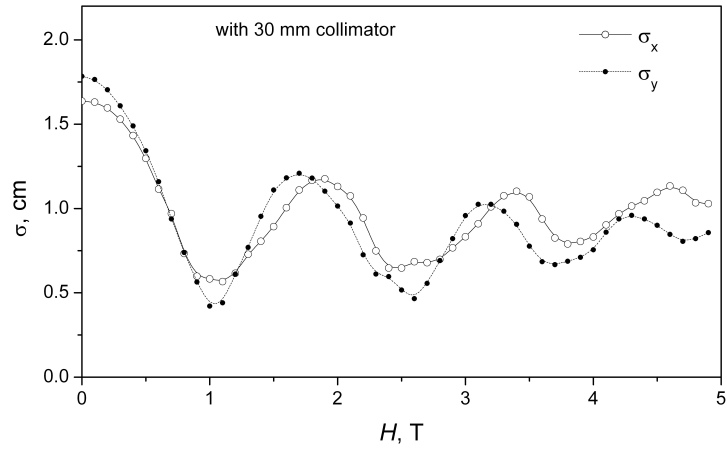


Figure 8: Dependencies of  $\sigma_x$  and  $\sigma_y$  (standard deviations for the X- and Y-distributions) on the magnetic field  $H$ : top – with 30 mm collimator; bottom – without collimator.

## Summary and Outlook

A position sensitive detector (the Muon Beam Profile Monitor) with avalanche microchannel photodiodes used for readout of scintillating fibers was developed. The  $\mu$ BPM was successfully utilized in the measurement of the magnetic field dependence of the muon beam profile in the center of a superconducting solenoid of the ALC-spectrometer and also for the commissioning of the new high-flux  $\mu$ E4 muon beamline. No deterioration of the device performance was observed in the fields up to 4.8 Tesla, or at muon rates as high as  $3 \cdot 10^6 \text{ s}^{-1}$  per channel.

The following improvements added to the design of the prototype presented in this work would be necessary for a state-of-the-art BPM:

- square cross-sections of the fibers (signal output independent of the muon trajectory in the fiber)
- increased number of channels (e.g., 20+20)
- on-board temperature controller
- on-board discriminators and logic circuits

## Acknowledgements

One of the authors (A.S) expresses his gratitude to Dr. D.Renker (PSI) and Dr. Yu.Musienko (CERN) for consultations on the operation of AMPDs.

This work was fully performed at the Swiss Muon Source ( $S\mu S$ ) at the Paul Scherrer Institut in Villigen, Switzerland, within the collaboration agreement between JINR and PSI on joint research in the field of "Development of scintillation detectors on the base of new microchannel avalanche photodiodes". The project has been supported by the European Commission under the 6th Framework Programme through the Key Action: Strengthening the European Research Area, Research Infrastructures. Contract no.: RII3-CT-2003-505925.

## References

- [1] <http://lmu.web.psi.ch/facilities/alc/alc.html>
- [2] The application of the ALC technique was first proposed in: A. Abragam, C.R. Acad. Sc. Paris **299** Series II, no. 3 (1984) 95. A detailed description and applications can be found, for example, in: E. Roduner, *Chem. Soc. Rev.* **22** (1993), 337 and references therein.
- [3] for the products of Pol.Hi.Tech see <http://www.polhitech.it/>
- [4] Z.Ya.Sadygov, V.N.Jejer, Yu.V.Musienko et.al., NIM A **504**, 301 (2003);  
<http://sunhe.jinr.ru/struct/neo/apd/>
- [5] for the products of Mini-Circuits see <http://www.minicircuits.com/>